

# Laser Imaging Nephelometer for aircraft deployment for FIREX-AQ

Adam T. Ahern<sup>1,2</sup>, Frank Erdesz<sup>1,2</sup>, Nicholas L. Wagner<sup>1,2\*</sup>, Charles A. Brock<sup>1</sup>, Ming Lyu<sup>3</sup>, Kyra Slovacek<sup>2,4</sup>, Richard H. Moore<sup>5</sup>, Elizabeth B. Wiggins<sup>5,6</sup>, and Daniel M. Murphy<sup>1</sup>

5 <sup>1</sup>NOAA Chemical Sciences Laboratory, Boulder, CO 80305, USA

<sup>2</sup>Cooperative Institute for Research in Environmental Sciences, University of Colorado, Boulder, CO 80309, USA

<sup>3</sup>Department of Chemistry, University of Alberta, Edmonton, AB T6G 2B4, Canada

<sup>4</sup>Civil, Environmental, and Architectural Engineering, University of Colorado, Boulder, CO 80309, USA

<sup>5</sup>NASA Langley Research Center, Hampton, VA 23666, USA

10 <sup>6</sup>NASA Postdoctoral Program, Universities Space Research Association, Columbia, MD 21046, USA

\*Now at Ball Aerospace, Westminster, CO 80021, USA

*Correspondence to:* Adam T. Ahern (adam.ahern@noaa.gov)

## Supplemental Information

Figure S1 shows a schematic of the laboratory setup for calibrating the Laser imaging nephelometer (LiNeph). In this  
15 configuration, the sample volume of the LiNeph can be evacuated and back-filled with calibration gases, either He or CO<sub>2</sub>.  
Alternatively, calibration aerosol may be introduced via positive pressure from a compressed zero air cylinder by removing  
the pump from the system and allowing the LiNeph to exhaust through the filter into the room.

Figure S2 shows the scattering angle calibration performed by matching maxima and minima observed in measured scattering  
intensity to the maxima and minima predicted by Mie theory. The calibration aerosol was atomized and dried polystyrene latex  
20 spheres of known size.

Figure S3 and Fig. S4 show a series of measurements from pure CO<sub>2</sub>. For this experiment, the LiNeph chamber was filled with  
CO<sub>2</sub> and then a series of images were captured. From these images, the He image was subtracted. Gaussian fits were applied  
to each pixel column. Figure S3 shows the area under that Gaussian fit for each image as a function of time for an individual  
pixel column, which corresponds to a scattering angle.

25 Figure S4 shows the standard deviation for the area under fitted Gaussian curves as a function of the average area under  
Gaussian curves for CO<sub>2</sub> measurements. The two traces show different exposure durations and have been normalized by CCD  
exposure time to be proportional to scattering intensity instead of the digital output. The spread in the data points is from  
additional noise due to stray light within the instrument. This illustrates that for measurements with abundant signal, the  
standard deviation is typically <2% of the average signal. But in cases of low signal, the standard deviation becomes constant  
30 ~200 bits<sup>2</sup>, and uncertainty is likely dominated by electronic noise. Since phase functions can span many orders of magnitude,  
we find it advantageous at times to increase the exposure time of the CCD, which linearly increases the signal while the  
electronic noise remains the same. The resulting Gaussian fit values can be scaled by their exposure time and recombined,  
allowing for more precise measurements of phase functions spanning multiple orders of magnitude.

Figure S5 shows the sum of all pixels while sampling a well-mixed smoke plume during FIREX-AQ. The red colored region indicates the period of the sampling when a filter is in the sampling line. Only the steady-state data points of the red region are used to correct for changing gas-phase scattering and instrument background light.

Figure S6 shows a subset of the plot on the right side of Fig. 6, showing only the data where the bridge dilution system was not being used, see Fig. 3. The greater linearity between the integrated scattering measured by the LiNeph and the AOP instrument suite for undiluted data compared to all data is consistent with the dilution system being an added source of uncertainty. This plot also indicates that there may be an error in the magnitude of the differential scattering calibration which results in the LiNeph measuring 20-30% more light scattering than what is observed by the AOP instrument suite. We do not expect this to influence the polarimetry measurements as they are normalized functions.

Figure S7 markers show the average normalized number-weighted size distributions for two transects during the Williams Flats Fire on August 7<sup>th</sup>, 2019. Each size distribution was first normalized by its maximum peak height. Then the average and standard deviation of each size bin was calculated for all the normalized size distributions from each transect. Size distributions were measured using the LAS with an ammonium sulfate calibration as discussed in Moore et al. (2021). Additionally, we fit each individual size distribution with a lognormal distribution and then calculated the average and standard deviation of the fitted mode. Transect 1 had an average mode of  $0.174 \pm 0.014 \mu\text{m}$  and Transect 10 had an average mode of  $0.225 \pm 0.011 \mu\text{m}$ .

50

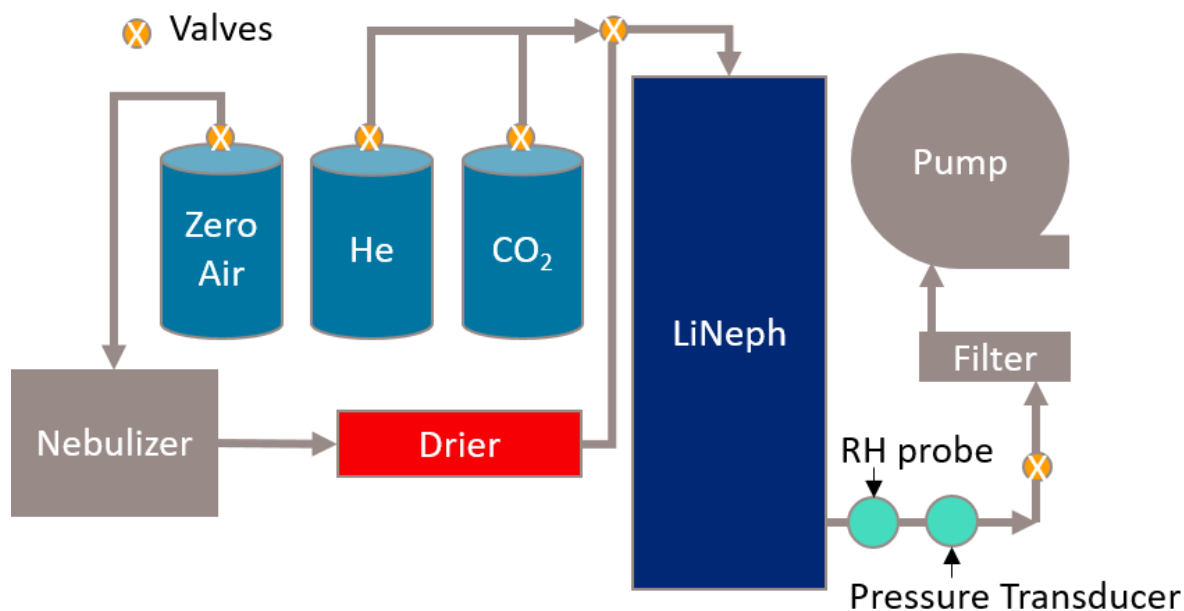
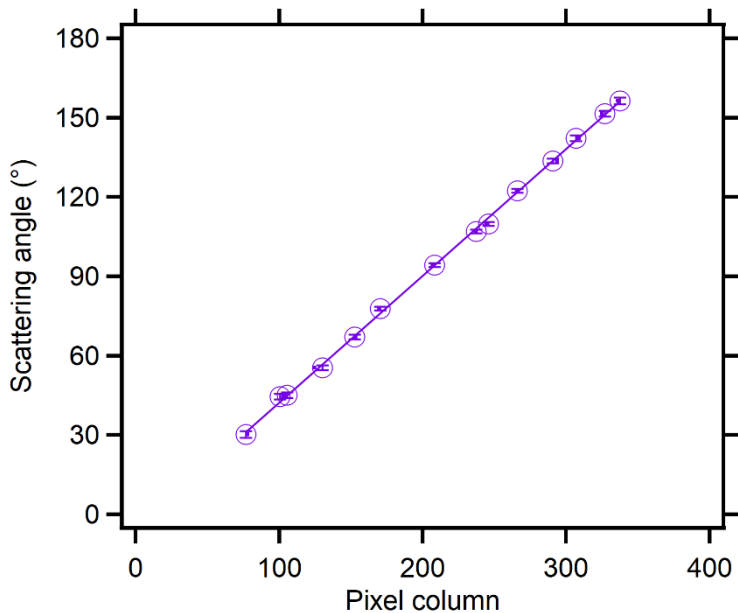
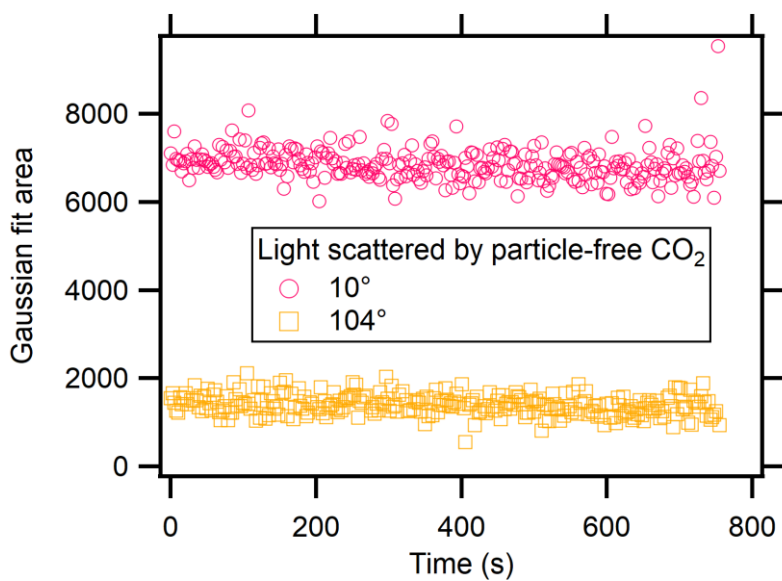


Figure S1. Diagram of laboratory calibration of Laser Imaging Nephelometer.



55 **Figure S2.** Calibration for converting pixels to scattering angles using PSL features.



**Figure S3.** Laser stability shown as area under Gaussian fit for light scattered by CO<sub>2</sub> at two scattering angles. Pink circles and yellow squares show individual measurements of light scattering at 10° and 104°, respectively, as a function of time.

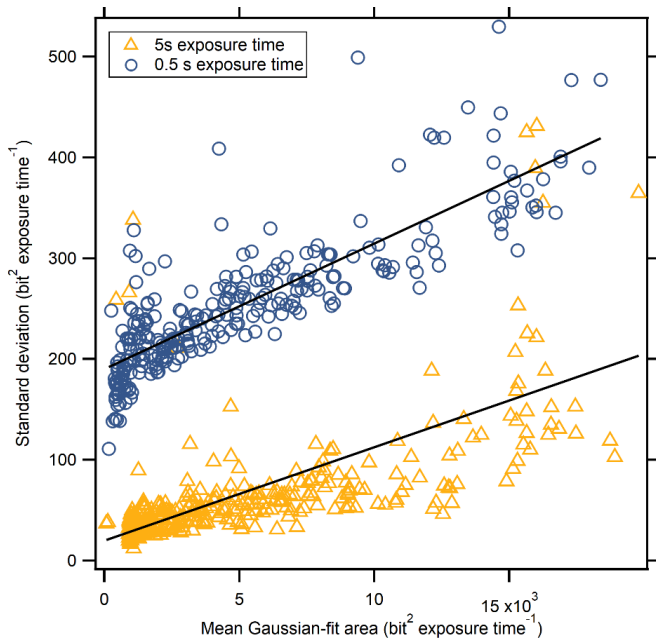


**Figure S4.** Standard deviation of area under Gaussian fit as a function of the average area under the Gaussian fit for two exposure durations. Each symbol represents a scattering angle for a series of measurements.

65

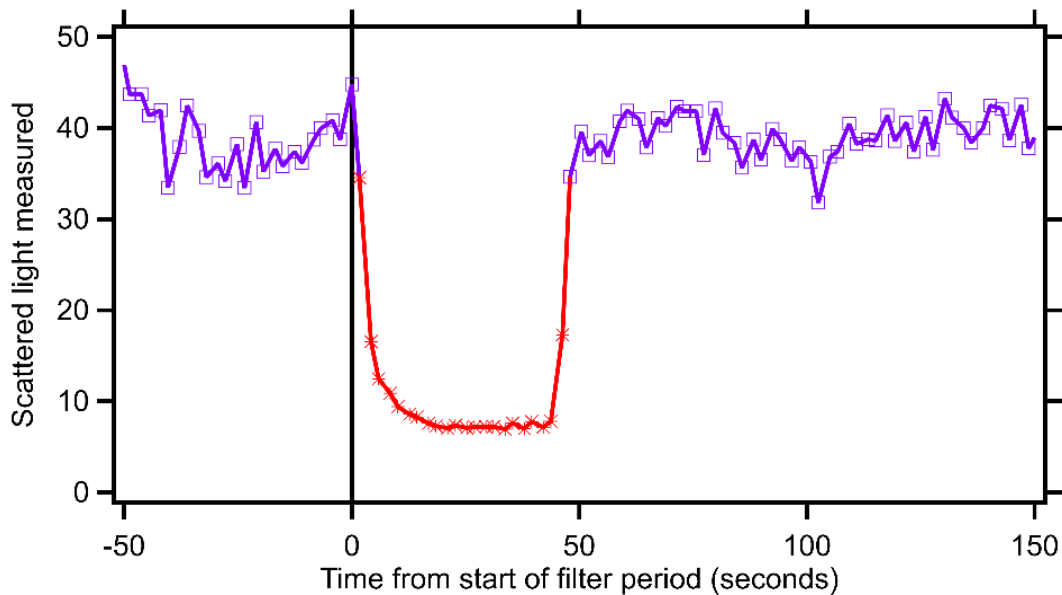
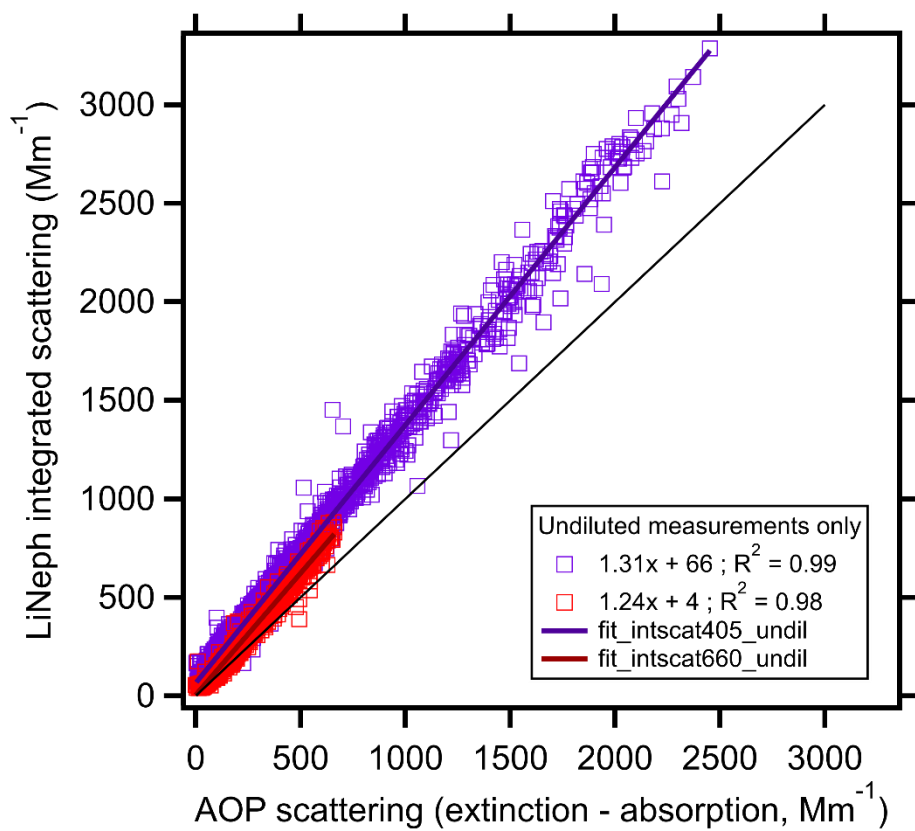
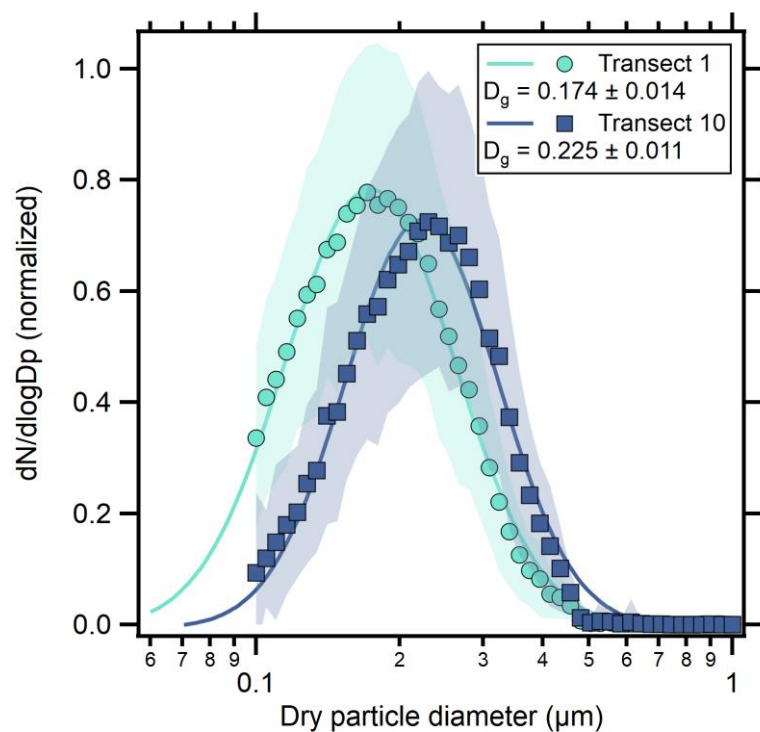


**Figure S5.** Change in light scattering after inserting a filter during smoke sampling. Red asterisks indicate the filter period and purple squares indicate sample data. Note: only steady-state data from the filter period is used for the subtraction of gas-phase scattering from the sample data.

70



75 Figure S6. Integrated scattering for undiluted measurements only.



80 **Figure S7.** Average normalized particle size distribution for two transects of the Williams Flats fire. Shaded area indicates one standard deviation from the average. The average  $\pm$  standard deviation geometric mean diameter ( $D_g$ ) is calculated from lognormal fits of each measured size distribution during each transect.